



Contents lists available at ScienceDirect

Vacuum

journal homepage: [www.elsevier.com/locate/vacuum](http://www.elsevier.com/locate/vacuum)

## Microstructural and magnetic characterization of ion-beam bombarded $[\text{Ni}_{80}\text{Fe}_{20}\text{-Cr}]_{50}$ thin films

Chao Zheng<sup>a</sup>, Ko-Wei Lin<sup>b,\*</sup>, Chi-Hsin Liu<sup>b</sup>, Hsun-Feng Hsu<sup>b</sup>, Chi-Wah Leung<sup>c</sup>, Wei-Hsien Chen<sup>d</sup>, Te-Ho Wu<sup>d</sup>, Ryan D. Desautels<sup>e</sup>, Johan van Lierop<sup>e,\*\*</sup>, Philip W.T. Pong<sup>a,\*\*\*</sup>

<sup>a</sup> Department of Electrical and Electronic Engineering, The University of Hong Kong, Pokfulam Road, Hong Kong

<sup>b</sup> Department of Materials Science and Engineering, National Chung Hsing University, Taichung 402, Taiwan

<sup>c</sup> Department of Applied Physics, Hong Kong Polytechnic University, Hung Hom, Hong Kong

<sup>d</sup> Graduate School of Materials Science, National Yunlin University of Science and Technology, Taiwan

<sup>e</sup> Department of Physics and Astronomy, University of Manitoba, Winnipeg R3T 2N2, Canada

### ARTICLE INFO

#### Article history:

Received 21 June 2014

Received in revised form

20 August 2014

Accepted 18 October 2014

Available online xxx

#### Keywords:

Ion-beam bombardment

Intermixing

Nano-composite

### ABSTRACT

Ion-beam bombardment during thin film deposition can effectively change the microstructure and thus influence the magnetic properties of the thin film system. In this paper, we studied plain (un-bombarded) and argon ion-beam bombarded multilayered  $[\text{Ni}_{80}\text{Fe}_{20}\text{-Cr}]_{50}$  thin films fabricated using a dual ion-beam deposition technique. The atomic force microscopy images of the bombarded thin films showed a much rougher surface and an increased average grain size. No noticeable exchange bias phenomenon was observed in the thin films deposited with or without bombardment, indicating that the interfacial uncompensated spins were prevented from providing the necessary unidirectional anisotropy due to interfacial intermixing. This significant intermixing between  $\text{Ni}_{80}\text{Fe}_{20}$  and Cr layers, and the etching process caused by the bombardment, led to the formation of a nano-composite  $[\text{Ni}_{80}\text{Fe}_{20}\text{-Cr}]_{50}$  thin film with a reduced Curie temperature. An enhancement of the coercivity attributed to the stronger NiFe–Cr coupling was also found, which was the result of additional pinning sites created by the bombardment. The bombarded thin film also exhibited a higher ZFC/FC divergence temperature compared to the un-bombarded film, which indicated a much stronger NiFe–Cr coupling and more coordinated alignment of the magnetization of the film's larger crystallites.

© 2014 Elsevier Ltd. All rights reserved.

### 1. Introduction

Ion-beam bombardment during the thin film deposition can change effectively the grain size distribution [1], crystallographic preferred orientation [2], and surface roughness [3] of film systems. Enhanced grain growth of Ge, Si, and Au films bombarded with different (silicon, argon, krypton, germanium, xenon) ion-beams has been reported [1]. Such enhanced grain growth was proportional to the ion-beam energy and weakly dependent on deposition temperature. In the study of interfacial exchange coupling in a

$\text{Ni}_{80}\text{Fe}_{20}/\text{NiO}$  system, Lin et al. found that the interface texture was altered from a random to striped conformation by increasing the ion current density [4]. A correlation between the tuned surface roughness caused by the low-energy ion-beam bombardment of the NiO layer and the thermal instabilities in the NiO crystallites was also observed [4]. These microstructural changes would consequently alter the magnetic properties of the thin film materials due to atomic intermixing, spin alignment, pinning, and different exchange coupling energies.

As a ferromagnetic (FM) material, permalloy ( $\text{Ni}_{80}\text{Fe}_{20}$ ) has been extensively used in the thin film industry due to its high permeability, low coercivity, and near-zero magnetostriction. Fassbender et al. investigated the magnetic damping behavior as a function of saturation magnetization in  $\text{Ni}_{80}\text{Fe}_{20}$  thin films [5]. By increasing the Cr ion implantation fluence, an enhancement of the (111) peak intensity, then a lattice expansion, and eventually amorphous  $\text{Ni}_{80}\text{Fe}_{20}$  thin films were created, which led to a decreased Curie

\* Corresponding author. Tel./fax: +886 4 22851068.

\*\* Corresponding author. Tel.: +1 204 474 6191.

\*\*\* Corresponding author. Tel.: +852 2857 8491; fax: +852 2559 8738.

E-mail addresses: [kwlin@dragon.nchu.edu.tw](mailto:kwlin@dragon.nchu.edu.tw) (K.-W. Lin), [johan@physics.umanitoba.ca](mailto:johan@physics.umanitoba.ca) (J. van Lierop), [ppong@eee.hku.hk](mailto:ppong@eee.hku.hk) (P.W.T. Pong).

temperature and saturation magnetization. More recently, the exchange bias [6,7] effects of NiFe/Cr-oxide bilayers were studied by Lin and Guo [8]. The exchange bias field ( $H_{ex}$ ) exhibited a linear dependence on the NiFe and Cr thicknesses. Also,  $H_{ex}$  was reduced by increasing Ar ion ratio during *in situ* bombardment of the film system deposition, implying that the defects could be created and consequently altered the FM order in Cr-oxide layer.

To further investigate the connection between the microstructure and magnetic properties, we studied  $[\text{Ni}_{80}\text{Fe}_{20}\text{-Cr}]_{50}$  multilayer thin films fabricated with ion-beam bombardment using different bombardment voltages (0 V, 150 V). It was found that the intermixing and etching processes caused by ion-beam bombardment effectively changed the microstructure of the thin films, which may also lead to a change of the spin structures in the thin films.

## 2. Experimental details

The  $[\text{Ni}_{80}\text{Fe}_{20}\text{-Cr}]_{50}$  thin films were deposited on amorphous  $\text{SiO}_2$  substrates by using a dual ion-beam deposition technique [9–11]. A Kaufman ion source (800 V, 7.5 mA) was used to direct an argon ion-beam onto a commercial  $\text{Ni}_{80}\text{Fe}_{20}$  or Cr target surface in order to deposit the  $\text{Ni}_{80}\text{Fe}_{20}$  or Cr layer. The  $\text{Ni}_{80}\text{Fe}_{20}$  and Cr layers were deposited alternately for 50 cycles. For the un-bombarded samples, the thicknesses of the  $\text{Ni}_{80}\text{Fe}_{20}$  and Cr layers was about 2 – 3 nm. For one multilayer system, an End-Hall ion source ( $V_{EH} = 150$  V) was used to *in-situ* bombard the film layer during the deposition process of the  $\text{Ni}_{80}\text{Fe}_{20}$  or Cr layer. No external magnetic field was applied during deposition. A JEOL (JEM-2010) transmission electron microscope (TEM) operating at 200 kV was used

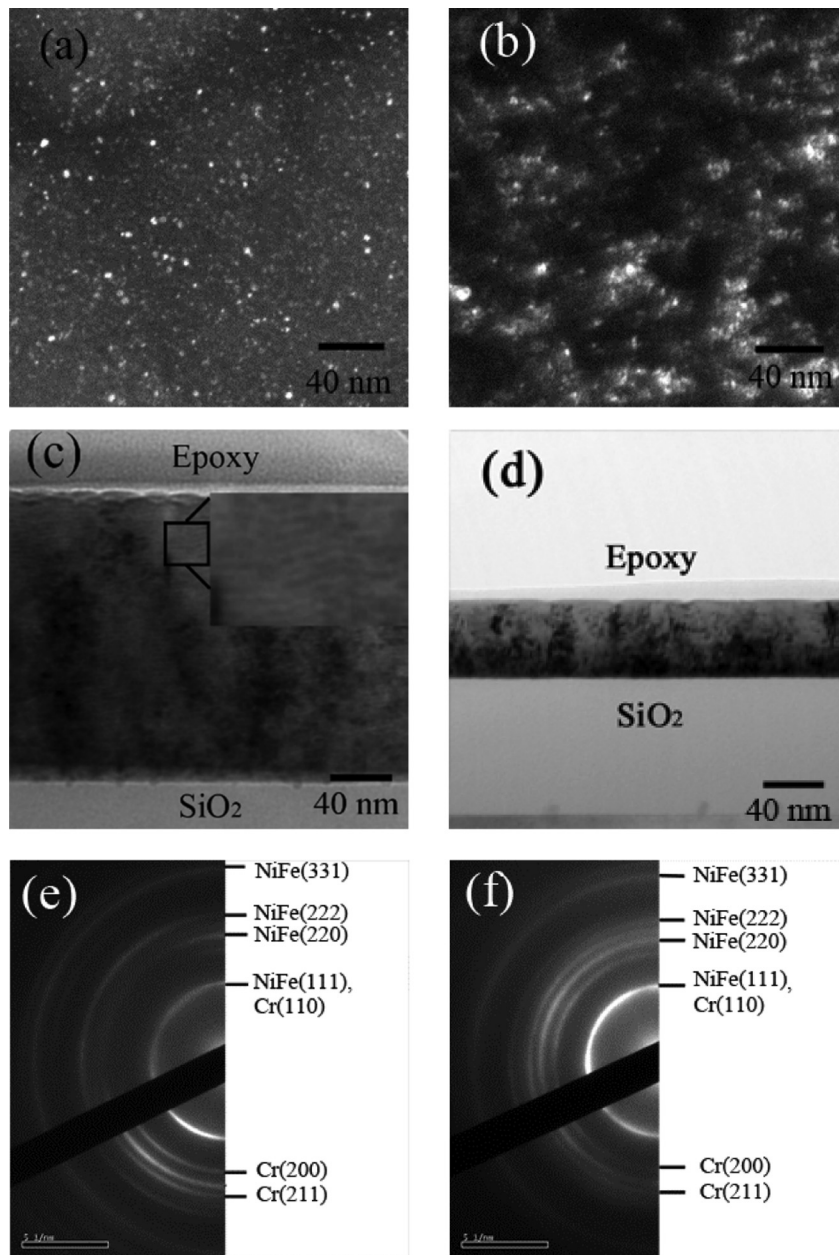


**Fig. 1.** Plane-view TEM micrographs of (a)  $[\text{Ni}_{80}\text{Fe}_{20}\text{-Cr}]_{50}$  thin film (without ion-beam bombardment during deposition,  $V_{EH} = 0$  V) and (b)  $[\text{Ni}_{80}\text{Fe}_{20}\text{-Cr}]_{50}$  thin film (with ion-beam bombardment during deposition,  $V_{EH} = 150$  V). The cross-sectional TEM images of both structures are displayed in (c) and (d). Corresponding electronic diffraction patterns for the un-bombarded and bombarded thin films are shown in (e) and (f), respectively.

for the microstructural analysis. In addition, a NTMDT Solver Pro-M atomic force microscopy (AFM) was used to measure the surface topography of the thin films. Then magnetic measurements were performed with a Quantum Design Magnetic Property Measurement System (MPMS) at 10 K and a Quantum Design vibrating sample magnetometer (VSM) at 160 K. The temperature dependence of the zero-field-cooled (ZFC) and field-cooled (FC)  $7.96 \times 10^3$  A/m DC magnetization ( $M$  vs  $T$ ) data of the thin films was measured with the MPMS.

### 3. Results and discussion

The microstructures of  $[\text{Ni}_{80}\text{Fe}_{20}\text{-Cr}]_{50}$  thin films are shown in the plane-view (Fig. 1a and b) and cross-sectional (Fig. 1c and d) dark-field TEM images. The planar-view images show the value of the mean grain size ( $\sim 5$  nm) in the thin film without bombardment ( $V_{\text{EH}} = 0$  V) which is smaller than that ( $\sim 15$  nm) with bombardment ( $V_{\text{EH}} = 150$  V) while the cross-sectional TEM images show a significant reduction of the film thickness with bombardment from  $\sim 250$  nm to  $\sim 65$  nm, indicating intermixing of  $\text{Ni}_{80}\text{Fe}_{20}$  and Cr and possibly an etching process caused by the bombardment. No superlattice structure was observed after the bombardment due to the intermixing between individual layers, as illustrated in Fig. 1d. The corresponding electron diffraction patterns for the un-bombarded and bombarded thin films are demonstrated in Fig. 1e and f, respectively. Both types of the samples consist of composite [f.c.c  $\text{Ni}_{80}\text{Fe}_{20}$  ( $a \sim 3.55$  Å), b.c.c Cr ( $a \sim 2.93$  Å)] phases. The presence of brighter diffraction rings for the bombarded sample suggests the growth of large crystal grains, coinciding with the results shown in the planar-view images.

Additionally, the mean grain size and roughness of the samples was measured by AFM (Fig. 2). These measurements were conducted over an area of  $1 \mu\text{m} \times 1 \mu\text{m}$ . Comparing Fig. 2a and c, one can observe a remarkable increase of the mean grain size after bombardment, which was consistent with the TEM results. It should also be noted that the bombarded surface ( $V_{\text{EH}} = 150$  V) (Fig. 2d) was much rougher than that ( $V_{\text{EH}} = 0$  V) (Fig. 2b) without

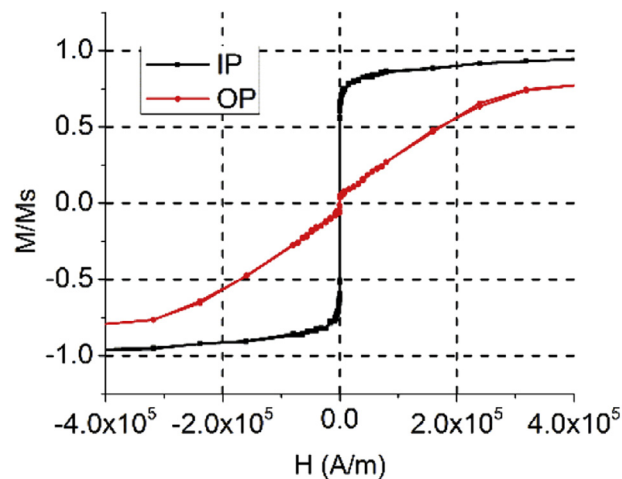


Fig. 3. In-plane (IP) and out-of-plane (OP) hysteresis loops of the plain  $[\text{Ni}_{80}\text{Fe}_{20}\text{-Cr}]_{50}$  thin films ( $V_{\text{EH}} = 0$  V) at 298 K.

bombardment as indicated by the root mean square (RMS) roughness parameters. Ion-beam bombardment process led to a significant increase of RMS roughness of the films from 0.56 nm ( $V_{\text{EH}} = 0$  V, Fig. 2b) to 2.58 nm ( $V_{\text{EH}} = 150$  V, Fig. 2d). This reveals that an etching effect occurred on the surface due to the bombardment, which also agreed with the results obtained by TEM.

Several representative hysteresis loops for  $[\text{Ni}_{80}\text{Fe}_{20}\text{-Cr}]_{50}$  thin films ( $V_{\text{EH}} = 0$  and 150 V) at the temperatures 298 K, 160 K and 10 K are displayed in Figs. 3–5, respectively. During the cooling process from 300 K to 10 K, an external magnetic field of  $7.96 \times 10^5$  A/m was applied. No noticeable exchange bias phenomenon was observed in the hysteresis loops, indicating that the uncompensated spins were prevented from providing the necessary unidirectional anisotropy due to interfacial intermixing in both types of the films. The dependence of  $H_{\text{C}}$  on the temperature for the un-bombarded and bombarded samples is shown in Fig. 6.

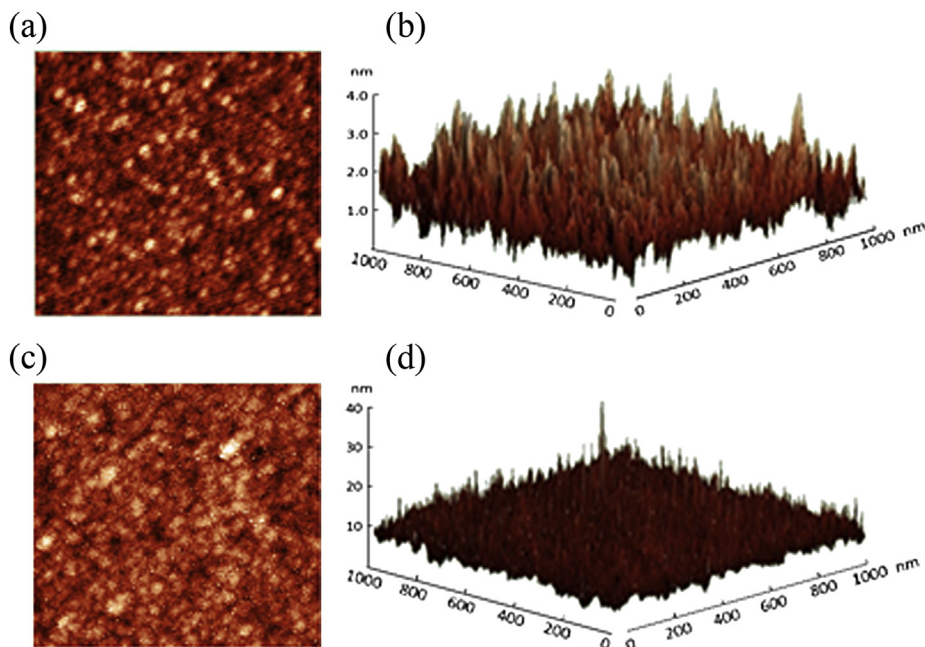
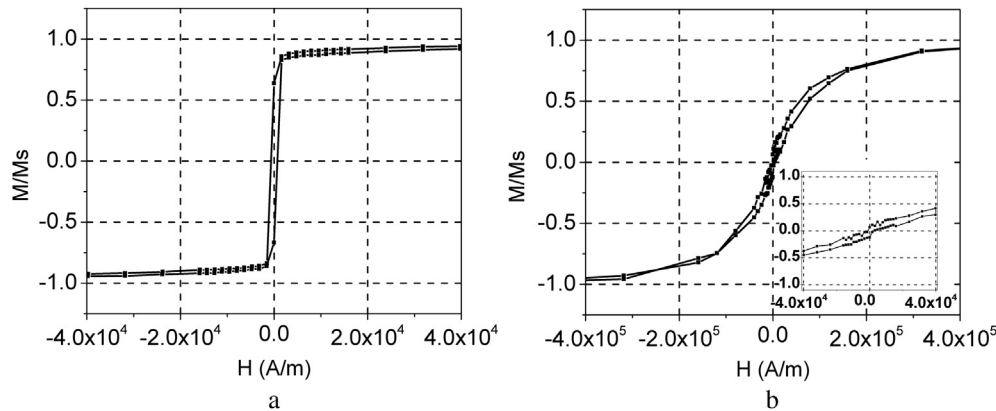
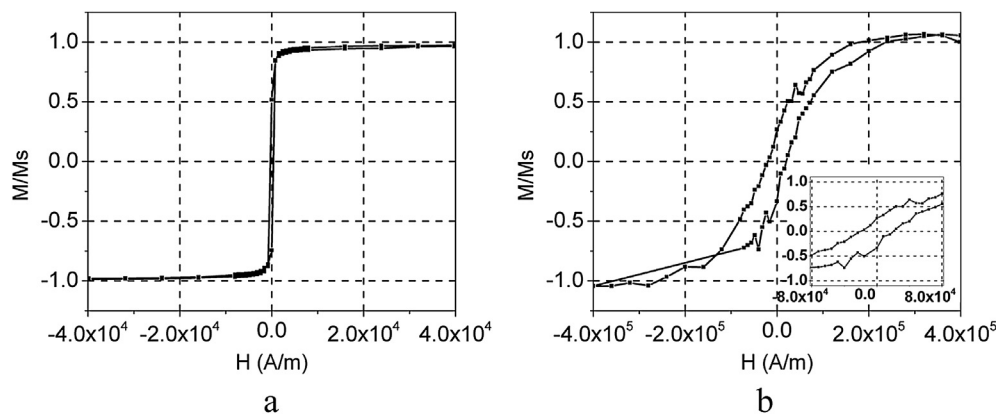


Fig. 2. AFM images of  $[\text{Ni}_{80}\text{Fe}_{20}\text{-Cr}]_{50}$  thin films ( $V_{\text{EH}} = 0$  and 150 V). Image area is  $1 \mu\text{m} \times 1 \mu\text{m}$ . Bombardment process resulted in root mean square (RMS) roughness increasing from 0.56 nm ( $V_{\text{EH}} = 0$  V, Fig. 2a and b) to 2.58 nm ( $V_{\text{EH}} = 150$  V, Fig. 2c and d).



**Fig. 4.** In-plane (IP) hysteresis loops of the  $[\text{Ni}_{80}\text{Fe}_{20}\text{-Cr}]_{50}$  thin films without (a) and with bombardment (b) at 160 K. The inset of (b) shows the IP loop for the bombarded sample with the magnetic field varying between  $-4 \times 10^4$  A/m to  $4 \times 10^4$  A/m.



**Fig. 5.** In-plane (IP) hysteresis loops of the  $[\text{Ni}_{80}\text{Fe}_{20}\text{-Cr}]_{50}$  thin films without (a) and with bombardment (b) at 10 K. The inset of (a) shows the IP hysteresis loop for the bombarded sample with the magnetic field varying between  $-8 \times 10^4$  A/m to  $8 \times 10^4$  A/m.

Both in-plane and out-of-plane hysteresis loops of the plain  $[\text{Ni}_{80}\text{Fe}_{20}\text{-Cr}]_{50}$  thin films were measured at room temperature (298 K) as shown in Fig. 3. The magnetization loops show the easy axis aligning along the in-plane direction for the un-bombarded thin film. This is evidenced by a narrow loop in the in-plane direction and a canted narrow loop in the out-of-plane direction. This thin film was magnetically soft and exhibited a small in-plane coercivity of 7.96 A/m. In contrast, no hysteresis was observed at room temperature for the bombarded thin film. This indicates that the intermixing between  $\text{Ni}_{80}\text{Fe}_{20}$  and Cr layers caused by the ion-beam bombardment led to the formation of a nano-composite  $[\text{Ni}_{80}\text{Fe}_{20}\text{-Cr}]_{50}$  thin film with a reduced FM ordering temperature [5,12]. This hypothesis was supported by the presence of a hysteresis loop for the  $[\text{Ni}_{80}\text{Fe}_{20}\text{-Cr}]_{50}$  ( $V_{\text{EH}} = 150$  V) thin film at 160 K (under an FC process) as shown in Fig. 4b. In other words, the bombardment effects suppressed the Curie temperature of the thin film to a certain value between 160 K and 298 K.

Fig. 4a and b shows the in-plane hysteresis loops of  $[\text{Ni}_{80}\text{Fe}_{20}\text{-Cr}]_{50}$  ( $V_{\text{EH}} = 0$  and 150 V) thin films at 160 K, respectively. As the temperature decreased from 298 K to 160 K, the value of coercivity for the un-bombarded sample increased from  $\sim 7.96$  A/m to  $\sim 716$  A/m (Fig. 6). It can be explained by the enhanced alignment of the interfacial FM and antiferromagnetic (AF) spins after the FC process. Such enhanced alignment strengthened the interaction between FM–AF spins at the interfaces and thus led to the larger coercivity [13,14]. After ion-beam bombardment, enhancement of coercivity from  $\sim 716$  A/m to  $\sim 2228$  A/m of the thin films was also found, which was likely derived from the additional pinning sites created

by the bombardment [5]. These pinning sites can inhibit the motion of domain wall and thus lead to a canted and unsmooth loop of the bombarded thin film (Fig. 4b). In addition, the small width of the hysteresis loop for the un-bombarded film indicates that the magnetization reversal of the  $\text{Ni}_{80}\text{Fe}_{20}$  phase can be attributed to the nucleation and growth of the reversible magnetic domains instead of the coherent rotation [15].

The in-plane hysteresis loops of the  $[\text{Ni}_{80}\text{Fe}_{20}\text{-Cr}]_{50}$  thin films measured at 10 K are shown in Fig. 5. For the  $[\text{Ni}_{80}\text{Fe}_{20}\text{-Cr}]_{50}$  thin film ( $V_{\text{EH}} = 0$  V), it was surprising to note that the coercivity experienced no change (Fig. 6), which requires investigation. On

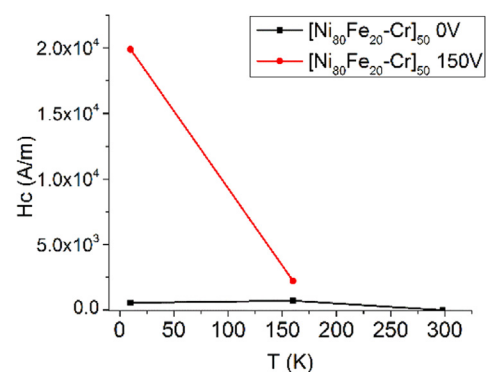


**Fig. 6.** The dependence of  $H_c$  on the temperature for the un-bombarded and bombarded samples. Error bars were smaller than the symbol size.



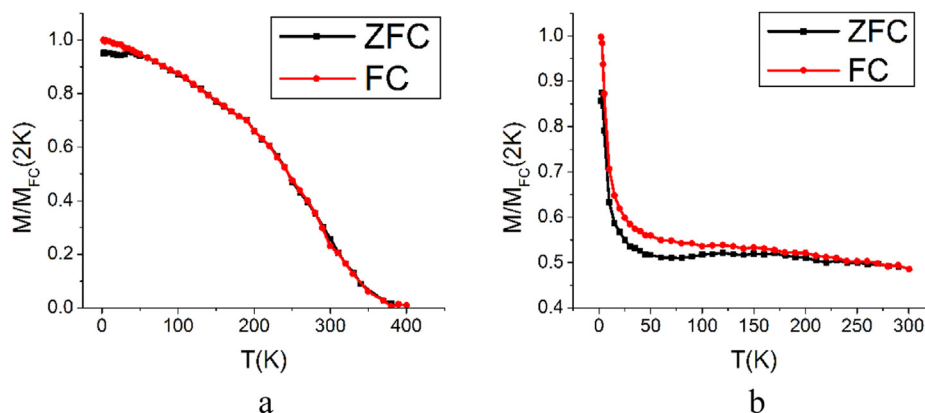


**Fig. 7.** Magnetization as a function of temperature for the  $[Ni_{80}Fe_{20}-Cr]_{50}$  thin films without (a) and with bombardment (b). Measurements were performed by zero-field-cooling the films from 400 K down to 10 K and using a  $7.96 \times 10^3$  A/m measuring field for the zero-field-cooled (ZFC) and field-cooled (FC) magnetization thermal scans. The “ $M_{FC}(2K)$ ” is the magnetization of the field-cooled thin films at 2 K.

the other hand, the bombarded thin film exhibited a significantly increased coercivity of  $\sim 1.99 \times 10^4$  A/m, which was much larger than that of the thin film without ion-beam bombardment. This indicates the interfacial pinning effect was strengthened at 10 K.

The dependence of magnetization ( $M$ ) as a function of the temperature ( $T$ ) was also measured. Fig. 7a and b shows the  $M-T$  data for  $[Ni_{80}Fe_{20}-Cr]_{50}$  ( $V_{EH} = 0$  V and 150 V) thin films, respectively. The measurements were performed by zero-field-cooling the films from 400 K down to 10 K and using a  $7.96 \times 10^3$  A/m measuring field for the zero-field-cooled (ZFC) and field-cooled (FC) magnetization thermal scans. In Fig. 7a, the  $[Ni_{80}Fe_{20}-Cr]_{50}$  ( $V_{EH} = 0$  V) ZFC  $M(T)$  curve exhibited a broad maximum at around 45 K, whereas the FC  $M(T)$  curve exhibited a constant increase from 400 K to 10 K, diverging from the ZFC  $M(T)$  at 45 K. This divergence is consistent with the spin reorientation transition in  $Ni_{80}Fe_{20}$  phase [E. Skoropata, K.-W. Lin, M. Plumer and J. van Lierop - unpublished results] and shows that the Cr layer was weakly coupled to the  $Ni_{80}Fe_{20}$  layer, in agreement with the hysteresis loop data discussed above. However, for the ion-beam damaged film that suffered significant intermixing (Fig. 7b), the ZFC/FC divergence temperature was increased to around 150 K, indicating a much stronger NiFe–Cr coupling and alignment of the magnetization of the film’s larger crystallites (e.g., larger thermal energies with warming required to thermally de-pin their respective magnetizations). Both ZFC and FC magnetizations showed a marked increase with temperatures below 25 K, implying a second smaller distribution of film crystallites was freezing with cooling, as indicated by the different microstructure and composition (e.g., etching effects) due to the ion-beam bombardment discussed above.

#### 4. Conclusions

In summary, the argon ion bombarding process can remarkably impact the microstructure and the magnetic properties of the  $[Ni_{80}Fe_{20}-Cr]_{50}$  thin films. Both the larger mean grain size and much rougher surface were observed after bombardment, which also led to a reduction of the Curie temperature. Furthermore, the coercivity of the bombarded thin film increased due to the enhanced NiFe–Cr coupling and improved alignment of the interfacial spins. To investigate the correlation between the microstructure and magnetic features, future work will focus on the effect of ion

bombardment on the formation and dynamics of magnetic domains.

#### Acknowledgments

This work was supported in part by NSC of Taiwan, NSERC of Canada, and the Seed Funding Program for Basic Research and Small Project Funding Program from the University of Hong Kong, ITF Tier 3 funding (ITS/104/13), RGC-GRF grant (HKU 704911P), and University Grants Committee of Hong Kong (Contract No. AoE/P-04/08).

#### References

- [1] Atwater HA, Thompson CV, Smith HI. Ion-bombardment-enhanced grain growth in germanium, silicon, and gold thin films. *J Appl Phys* 1988;64: 2337–53.
- [2] Okuno SN, Hashimoto S, Inomata K. Preferred crystal orientation of cobalt ferrite thin films induced by ion bombardment during deposition. *J Appl Phys* 1992;71:5926–9.
- [3] Eklund EA, Bruinsma R, Rudnick J, Williams RS. Submicron-scale surface roughening induced by ion bombardment. *Phys Rev Lett* 1991;67:1759.
- [4] Lin KW, Mirza M, Shueh C, Huang HR, Hsu HF, Van Lierop J. Tailoring interfacial exchange coupling with low-energy ion beam bombardment: tuning the interface roughness. *Appl Phys Lett* 2012;100:122409–14.
- [5] Fassbender J, Von Borany J, Mücklich A, Potzger K, Möller W, McCord J, et al. Structural and magnetic modifications of Cr-implanted permalloy. *Phys Rev B* 2006;73:184410.
- [6] Stiles MD, McMichael RD. Model for exchange bias in polycrystalline ferromagnet-antiferromagnet bilayers. *Phys Rev B* 1999;59:3722–33.
- [7] Nogués J, Schuller IK. Exchange bias. *J Magn Magn Mater* 1999;192:203–32.
- [8] Lin KW, Guo JY. Tuning in-plane and out-of-plane exchange biases in NiFe/Cr-oxide bilayers. *J Appl Phys* 2008;104:123913.
- [9] Johansson B, Hentzell H, Harper J, Cuomo J. Higher nitrides of hafnium, zirconium and titanium synthesized by dual ion beam deposition. *J Mater Res* 1986;1:442.
- [10] Su HC, Huang MJ, Lin HJ, Lee CH, Chen CT, Liu CH, et al. Connection between orbital moment enhancement and exchange bias in a  $[Ni_{80}Fe_{20}/Mn]_3$  multilayer. *Phys Rev B* 2013;87:014402.
- [11] Liu CH, Shueh C, Lan TC, Lin KW, Chen WC, Wu TH, et al. Unusual exchange bias effects induced in NiFe/Mn thin films via ion-beam bombardment: superlattice vs nanocomposite. *J Korean Phys Soc* 2013;62:1958–62.
- [12] Chakraborty S, Mukherjee G, Rathnayaka K, Naugle DG, Majumdar A. Low-temperature magnetization in Ni-rich  $\gamma-Ni_{100-x}Fe_xV_y$  alloys. *Phys Rev B* 2000;62:476.
- [13] Leighton C, Noguez J, Jonsson-Akerman B, Schuller IK. Coercivity enhancement in exchange biased systems driven by interfacial magnetic frustration. *Phys Rev Lett* 2000;84:3466.
- [14] Scholten G, Usadel KD, Nowak U. Coercivity and exchange bias of ferromagnetic/antiferromagnetic multilayers. *Phys Rev B* 2005;71:064413.
- [15] Jiang JS, Felcher GP, Inomata A, Goyette R, Nelson C, Bader SD. Exchange-bias effect in Fe/Cr(211) double superlattice structures. *Phys Rev B* 2000;61: 9653–6.